4th INTUITION International Conference on Virtual Reality and Virtual Environments proceedings
4-5 October 2007, Athens, Greece
ISBN-978-960-254-665-9
Institute of Communication and Computer Systems of the National Technical University of Athens, 2007

# Wearable Haptic Glove with McKibben Actuators and Optical Tracking for Virtual Environments

**Jukka Kuusisto[1], Tuukka Takala[2], Otto Korkalo[2], Asko Ellman[1], Tapio Takala[2]**

(1) Institute of Machine Design,
Tampere University of Technology, PL 589, FIN-33101, Tampere, FINLAND
E-mail: jukka.kuusisto@tut.fi
(2) Telecommunications Software and Multimedia Laboratory,
Helsinki University of Technology, Konemiehentie 2, Espoo, FINLAND

**Abstract**

*For touching and manipulating objects in virtual environments conveniently, wearable haptic interfaces are required. In this paper, a concept of combining a McKibben pneumatic muscle based wearable haptic glove with an optical hand tracking system is presented. Dynamic characteristics of the muscle are measured as well as the static accuracy of the tracking system. The results are discussed, and possible improvements are considered. In addition to this, the concept of finger tracking is examined, and its integration to our system is given thought.*

**Keywords**: Wearable haptics, Optical tracking, McKibben actuator, Hand tracking

## 1 Introduction

The haptic sense plays an important role in human interaction with virtual environments. In order to get a realistic feeling of touching and manipulating virtual objects, a haptic device is needed for generating feedback to the user. Because free movement in the virtual environment is a valuable asset, the haptic system should be wearable. Tracking the location and orientation of the user's hand is required so that touching a virtual object can be detected and haptic feedback can be generated. Tracking can be implemented with several different approaches such as electromagnetic, acoustic, inertia-based and optical methods. From the point of view of free movement for the user, optical tracking systems are beneficial because they are wireless. In this paper, a concept of combining a wearable McKibben muscle based haptic glove with an optical tracking system is presented and its performance is measured and analysed.

### 1.1 Wearable Haptics

Haptic interfaces can be divided into grounded and portable implementations. Due to the desire for free movement, our focus is on portable and especially wearable devices. Wearable artificial force displays often have a backpack-type mechanism to minimize fatigue for the wearer, as for example in HapticGEAR, which relays force to the user via a wire tension mechanism and the force can be felt at the tip of a pen-type grip (Hirose *et al*, 2001).

Glove-like designs are practical for applications that involve touching and manipulating virtual objects by hand in virtual environments. Usually an exoskeleton is used to transfer the feedback signal mechanically to the user's body. Commercial implementations on this field exist, such as

ISBN-978-960-254-665-9


Immersion Corporation's CyberGrasp (Immersion, 2007). The Rutgers Master II-ND glove uses direct-drive pneumatic actuators in the palm, which allows the structure to be compact and light (Bouzit *et al*, 2002). In Tampere University of Technology, a wearable force-reflecting exoskeleton was developed. It applied forces to four fingers and was actuated by DC motors. Motor positions were measured by incremented optical encoders and forearm position and orientation by an Ascension Bird motion tracker (Iltanen and Ellman, 2005; 2007).

### 1.2 McKibben Pneumatic Muscle

The McKibben pneumatic muscle consists of an internal expanding tube surrounded by flexible but non-extensible braided cords. When the tube is pressurized, its volume increases and the properties of the cord threads cause the actuator to shorten according to its volume increase. Thus, tension is produced when the muscle is connected to a mechanical load. Typically, the actual achievable contraction of the muscle without load is 30 % of the nominal length. With advanced controllers, displacement accuracy of 1 % is achievable (Caldwell *et al*, 2000). The McKibben muscles have variable-stiffness spring-like characteristics and nonlinear passive elasticity. In addition, they are physically flexible and reasonably light. These properties make the McKibben muscle suitable for wearable haptic devices. (Chou and Hannaford, 1996)
In this research, the Festo fluidic muscle, depicted in Figure 1, is used (Festo, 2007). It is slightly different from the general McKibben type muscles in that the fibre of the fluidic muscle is knit in the tube itself. This configuration offers some advances like easy assembling, improved hysteretic behaviour and non-linearity. The force generated by the muscle decreases with increasing contraction and is an almost linear function of pressure when contraction is kept at a constant value (Jouppila and Ellman, 2006).

*Figure 1. Festo fluidic muscle.*

### 1.3 Optical Tracking

Magnetic tracking has some downsides such as it requires an additional wire to be connected to the user and it is disturbed by ferromagnetic substances. Optical tracking overcomes these issues. Optical tracking can be based on either fiducial markers or natural features. An example of marker-based tracking is ARToolKit (ARToolKit, 2007), where square-shaped planar markers are used for pose calculations (Woods *et al,* 2003). Marker-based head tracking has been implemented in several ways, such as by attaching a triangular planar marker to VR glasses and estimating the pose of the marker using calibrated stereo pair and standard epipolar geometry (Mulder *et al,* 2003), or estimating the pose of a rigid 3D set of retro reflective balls using monocular video (Mathieu, 2005). Optical hand tracking was implemented by Duca et al. who applied square markers and a single webcam, adding lines to user's fingers for additional information on the position of fingertips (Duca *et al,* 2007).

## 2 Haptic Glove with McKibben Actuators

The exoskeleton structure of the glove is made of plastic. The pneumatic muscles have a diameter of 10 mm and length of 150 mm (60 mm for the thumb) and they are attached to the exoskeleton. Each muscle is controlled by a separate pressure regulator (Festo MPPES-3-1/8-6-420). The pressure regulators are located in the backpack. The tubes between the regulators and muscles are approximately 1 m long and have an inner diameter of 2.5 mm. In the first

ISBN-978-960-254-665-9
Institute of Communication and Computer Systems of the National Technical University of Athens, 2007

prototype (Figure 2), the structure is quite robust due to the size of the muscles used. In the future, smaller McKibben muscles will be manufactured and the exoskeleton made lighter.

*Figure 2. First prototype of haptic glove with McKibben muscles.*

The functioning of the haptic glove has been tested in virtual environment together with the Virtools visualization software. At this stage, the pneumatic muscles were controlled with simple on/off-signals and magnetic tracking was used to detect hand and finger positions.

The dynamic characteristics of the muscles are analysed by measuring the step responses with regard to pressure and displacement. The measurements are conducted with an unloaded muscle, as the load caused by fingers in actual use is quite small. Five step signals of different levels (2–6 bars) are input to the pressure regulator and a pressure sensor and an LVDT sensor are used to measure the muscle pressure and displacement responses.

# 3 Overview of the Optical Tracking System

We implemented a marker based optical tracking system to capture user hand poses. Our system tracks a flat marker object with a predefined, asymmetric 2D pattern (Figure 3), which is attached on the back of user's hand. This tracking system can use one or more infra-red sensing cameras to track the location and orientation (six degrees of freedom) of several different marker objects. When the marker is seen by at least one camera, its pose relative to the camera can be calculated from the 2D pattern. Additional cameras will increase the accuracy and tracked area size. Our current data fusion implementation simply averages the location and orientation samples if the marker is seen by several cameras.

*Figure 3. A view from tracker camera, showing the marker features.*

The tracking method used here is based on planar homographies. This approach to pose estimation was presented by Prince et al. (Prince *et al,* 2002) in context of augmented reality applications. Based on the work by Zhang (Zhang, 2000), we estimate the marker pose from the homography between the marker pattern and camera image plane. Our current patterns for markers are groups of dots arranged in a circle formation, where one dot differs from the others to create asymmetry, which is required for orientation tracking. The detected dot centroids are used to approximate the circle pose in the camera image plane, which in turn can be used to estimate the marker pose.

Our tracking application iterates the following procedure:

1) Captured grey-scale camera image is thresholded into a binary image.
2) Connected components (blobs) are found and accounted for from the binary image.
3) The blobs are filtered to find the marker and its dots.

ISBN-978-960-254-665-9
Institute of Communication and Computer Systems of the National Technical University of Athens, 2007

4) Centroids for each dot are estimated.
5) The marker circle pose in the camera image plane is estimated from the dot centroids.
6) The homography between the marker and camera image plane is estimated from the circle pose.
7) Based on the homography, a rigid transformation matrix between the marker and camera is calculated.
8) The rigid transformation matrix containing the marker pose is refined with non-linear optimization.

The camera image plane is connected to real world coordinates via intrinsic and extrinsic camera parameters. Intrinsic parameters describe the different internal properties of the camera, such as focal length and lens distortion. Extrinsic parameters on the other hand comprise of camera location and translation in the real world. Before employing our tracker, we do a one-time calibration of cameras using OpenCV's (Intel, 2007) extended pinhole model implementation to find out the intrinsic parameters. After this, setting the tracker world coordinate system is very straightforward in our implementation: When the marker is seen by all cameras (the extrinsic parameters for each camera are known), the coordinates can be fixed with a single key press, placing the origin into the marker location. The coordinates of that setup are valid until the cameras are moved. This allows easy realignment of cameras and work space without further time-consuming calibration.

To avoid many problems of colour based tracking, the cameras in our setup are calibrated to be more sensitive for near infra-red spectrum. The markers are made of retro reflective materials, and lit by near infra-red LEDs placed next to each camera. With additional camera exposure settings, the cameras see only the lit marker pattern, with minimal disturbance from other factors, such as user movement. Figure 3 is a captured image from one of the tracker cameras, taken in a normal office lighting, while the marker was lying on a wooden table alongside with paper sheets and metal rulers.

We have already made initial tests with our hand pose tracker combined with commercial data gloves, which output finger pose information. The initial results suggest that a user interface based on hand gestures and movement can be successfully used to control Blender, a open source 3D modelling and animation tool.

To become independent of clumsy and rare data gloves, we plan to implement optical finger tracking in the near future. There are several approaches, with particle filters being one possibility to solve finger poses. The latest methods, such as Smart Particle Filtering (SPF) by M. Bray et al. (Bray *et al*, 2007), still take several seconds to process a single frame with a hand model of 26 degrees of freedom. While this is too slow for real time applications, we don't want to outright dismiss these methods however.

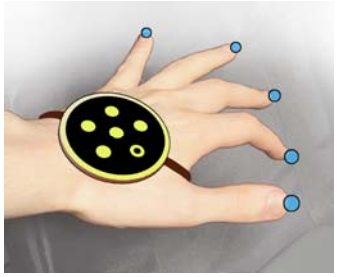

*Figure 4. Concept of hand pose tracking combined with finger tracking.*

One promising approach is by Duca et al. (Duca *et al,* 2007), who have developed hand tracking similar to ours combined with finger tracking which provides two degrees of freedom for each finger. We consider adopting a similar implementation, by replacing the colored finger markers with retroreflective material. This would allow us to use our existing infra-red based implementation.

ISBN-978-960-254-665-9
Institute of Communication and Computer Systems of the National Technical University of Athens, 2007

A tentative finger tracking concept is illustrated in Figure 4, in which finger poses are crudely estimated from the hand pose and fingertip marker locations. Combining this kind of finger tracking with our haptic device and a 3D modelling application should provide interesting results.

# 4 Results

In this section, the results of measuring the performance of both the McKibben pneumatic muscles as well as the optical tracking system are presented.

## 4.1 Dynamic Characteristics of the Pneumatic Muscle

The measurement results are presented in Figure 5.

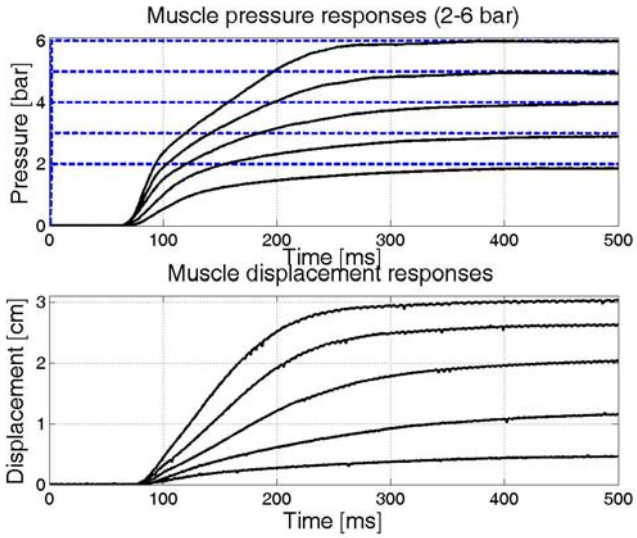


*Figure 5. Measurement results of the pneumatic muscle.*

The first thing to be noticed is the delay of approximately 75 ms before the pressure starts to rise in the muscle. This is caused by the slowness of the pressure regulator as well as the length of tubing that has to be filled with air before the air flow reaches the muscle. By using a faster regulator and reducing the amount of excess tubing, this delay can be minimized.

The time constant $\tau$ can be estimated from the measurements as the time required for the muscle displacement to rise to the −3 dB (≈ 63 %) point. As can be seen from Table 1, the average cut-off frequency for different supply pressures is approximately 1.4 Hz.

*Table 1. Characteristics of muscle displacements for different pressure levels.*

| Supply pressure | Time constant $\tau$ | Cut-off frequency $1/\tau$ |
|---|---|---|
| 6 bar | 84 ms | 1.9 Hz |
| 5 bar | 104 ms | 1.5 Hz |
| 4 bar | 126 ms | 1.3 Hz |
| 3 bar | 139 ms | 1.1 Hz |
| 2 bar | 126 ms | 1.3 Hz |

## 4.2 Hand Tracking Measurement Setup

Currently our tracking system consists of two infra-red sensing, monochromatic Unibrain Fire-i digital board cameras, both operating at 30 frames per second with resolution of 640×480. We run our tracking application on Windows XP using a standard desktop PC with 2.8 GHz Pentium 4 CPU and 1 GB of memory.

We conducted static accuracy measurements in three different predetermined poses ('Pose 0', 'Pose 1' and 'Pose 2'). Cameras were placed behind the upper left and right side of a standard

ISBN-978-960-254-665-9


office table, which was used as the xy-plane in terms of measurement coordinates. This camera setup was able to track an exemplar working area of the intended user, with approximate dimensions of width 80 cm, depth 40 cm and height 40 cm.
The marker poses were selected so that that they were seen by both cameras at the same time while keeping the distance from cameras within 80 to 110 cm during the measurement. In every pose the marker pattern size stayed between 0.4 %–0.9 % of the total 640×480 pixels on both camera image planes. The placement of the marker into each pose was done by hand with the aid of rulers. The measurement coordinate system was calibrated so that marker Pose 0 defined the origin and the direction of x-, y- and z-axes. Pose 1 was 25 cm in +x direction with rotation of 180 degrees around z axis. Pose 2 was 40 cm in +y direction with rotation of −45 degrees around z-axis (Figure 6).

*Figure 6. The measurement setup while tracking 'Pose 2'.*

While there was a ±0.5 mm location uncertainty in the placement of marker for each pose on all axes, the main concern was about inaccuracies in the marker itself, which resulted from the marker being constructed by cutting pieces of retro reflective material and placing them by hand on a printed marker template. Much care went into aligning the marker for Pose 0, so that the x- and y-axes defined by the marker would have been aligned with the measurement x- and y-axes on the table, because this precision affects the systematic error in other poses.
This narrow set of poses was chosen partly because of practical limitations such as time and ease of measurement setup, and partly because our current implementation easily loses track of the markers, if they are in too steep an angle when compared to camera view direction.
The actual measurements for each pose were done by storing 100 sequential samples of marker location and orientation in real time from the tracker. The orientation data was stored as rotation matrices, and then converted into quaternions, so we could use a simple metric to calculate rotational variation.

### 4.3 Hand Tracking Accuracy

The measurement results can be seen from Table 2, which illustrates the spatial jitter, and from Table 3, which contains the sample mean and standard deviation for spatial and angular components of the poses. In Table 2, the left and right rows have respectively the 2D and 3D plots of the different marker locations. The 2D plots illustrate the jitter in x and y directions. The view of the 3D plots are selected in way which reveals that the marker location samples lie on planes, whose normals are drawn with green lines. Individual samples are shown as blue dots, and the green square represents their average. Red dots show the location where the markers were placed in the real world coordinates, excluding Pose 1, which was too far away considering sensible plotting. Examining Table 2, we see that the spatial jitter happens on a 2D disc with a radius of 1 mm at most. Using principal components analysis, the normal of the disc is found to be the same as of the plane, which is formed by the two camera locations and the

ISBN-978-960-254-665-9
Institute of Communication and Computer Systems of the National Technical University of Athens, 2007

marker. This result suggests that our tracking method has the most jitter in directions, which are perpendicular to camera image planes.

In Table 3, the location of the marker is presented as it was in the real world, alongside with the mean and standard deviation of the samples, which were obtained from the tracker. The orientation of the marker is presented similarly, first in the real world, and then as seen by our tracker. The orientation is presented in quaternions, which were selected for obtaining continuous rotational function, necessary for correct standard deviation calculations. For reader convenience, the corresponding orientations are presented also in Euler angles. Examining mean values of location from Table 3, a somewhat significant systematic error can be found. In Pose 1, when the marker is 25 cm from the origin, the tracked sample mean is 6 mm off from the intended location. In Pose 2, when marker is 40 cm from the origin, this offset in mean is 7 mm. The angular standard deviation suggests that angular jitter is insignificant in all three poses. Looking at all the poses, angular systematic error in Euler γ-angle stays within the estimated marker placement uncertainty of ±1.0 degrees. On other angles the systematic error is at most 1.4 degrees. It should be noted that the quaternion mean values in Table 2 are not normalized.

*Table 2. Measurement results for hand tracking accuracy.*

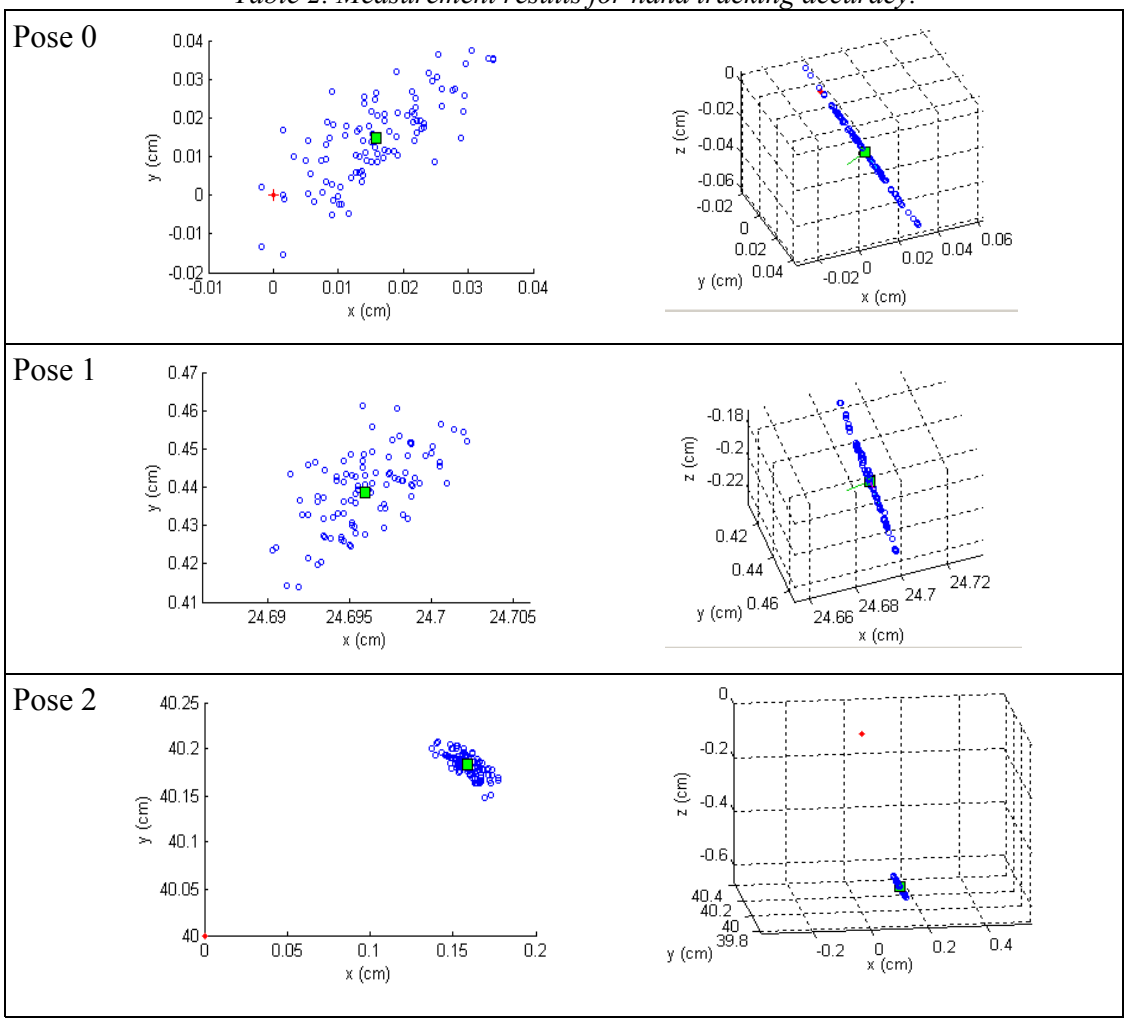

ISBN-978-960-254-665-9
Institute of Communication and Computer Systems of the National Technical University of Athens, 2007

*Table 3. Data sheet revealing the jitter and systematic error when tracking poses.*

| | **Real world** | **Tracker mean** | **Tracker standard deviation** |
|---|---|---|---|
| **Pose 0** | | | |
| x, y, z: (cm) | 0, 0, 0 | 0.02, 0.01, -0.03 | 0.008, 0.011, 0.015 |
| $q_t$, $q_x$, $q_y$, $q_z$ | 1, 0, 0, 0 | 1.0000, -0.0002, 0.0003, -0.0001 | ( 0.000, 0.352, 0.317, 0.157 ) * $10^{-3}$ |
| α, β, γ: (degrees) | 0, 0, 0 | 0.20, -0.39, 0.01 | 0.04, 0.04, 0.02 |
| **Pose 1** | | | |
| x, y, z: (cm) | 25, 0, 0 | 24.70, 0.44, -0.20 | 0.003, 0.010, 0.013 |
| $q_t$, $q_x$, $q_y$, $q_z$ | 0, 0, 0, 1 | 0.009, 0.012, 0.011, 1.000 | ( 0.082, 0.299, 0.225, 0.005 ) * $10^{-3}$ |
| α, β, γ: (degrees) | 0, 0, 180 | -1.3, 1.4, 181.0 | 0.03, 0.03, 0.02 |
| **Pose 2** | | | |
| x, y, z: (cm) | 0, 40, 0 | 0.16, 40.18, -0.63 | 0.009, 0.012, 0.015 |
| $q_t$, $q_x$, $q_y$, $q_z$ | 0.924, 0, 0, 0.383 | 0.925, 0.004, 0.008, 0.381 | ( 0.037, 0.183, 0.168, 0.092 ) * $10^{-3}$ |
| α, β, γ: (degrees) | 0, 0, -45 | -0.8, -0.7, -44.8 | 0.03, 0.03, 0.02 |

# 5 Conclusions and Discussion

The human muscle like properties of the McKibben actuator make it suitable for wearable haptic devices. The measurements of the dynamic characteristics of the muscle showed that a faster pressure regulator is needed and the amount of excess tubing should be minimized to make the muscle responses faster. The usability of the concept will be evaluated when the haptic glove is combined with the optical tracking system and user tests can be conducted.

The static accuracy of our hand pose tracker appears to be sufficient for a hand controlled user interface: The location jitter stays within a disc of 1 mm radius at most, while the maximum systematic error is 7 mm after moving the marker 40 cm away from the origin. The angular jitter is negligible, and the angular systematic error is less than 1.5 degrees.

We acknowledge that these measurements say very little about dynamic situations, in which movement of the marker causes motion blur thus reducing the accuracy. We are however satisfied with the accuracy in our preliminary tests with moving markers.

When going through the above measurements, some problems in our tracking implementation were found. Our infra-red LEDs don't have a wide enough light cone, and the tracker quickly stops recognizing the marker pattern in dim infra-red lighting, if the marker is placed near the edge regions of camera view, or if the pattern surface is in too steep an angle compared to the camera view direction. The current marker pattern is also a little too complicated for our resolution of 640×480, since the tracking fails if the marker is place over 1.5 meters away from the cameras. A simpler pattern would also be easier to construct precisely, hopefully making the tracker more accurate.

In the future, we plan to address the shortcomings of our current tracker, and implement an optical finger tracker on top of it. We also plan to attach more cameras into our system, so that on average one or two cameras see the markers at all times.

To further increase the accuracy of our tracker, we will investigate the fields of Kalman filtering and data fusion. One idea is to use such a Bayesian data fusion, which places more uncertainty for location information in the direction of the camera view axis, and then fuses the marker location probability distributions of different cameras in some optimal sense.

ISBN-978-960-254-665-9


# 6 References

## 6.1 Journal Articles

Bouzit, M., Burdea. G., Popescu, G. and Boian, R. (2002): The Rutgers Master II — New Design Force-Feedback Glove. *IEEE/ASME Transactions on Mechatronics 7*, 2, 256–263.

Bray, M., Koller-Meier, E. and Van Gool, L. (2007): Smart Particle Filtering for High-Dimensional Tracking. *Computer Vision and Image Understanding, Springer LNCS,* in press.

Caldwell, D.G., Tsagarakis, N. and Medrano-Cerda, G.A. (2000): Biomimetic Actuators: Polymetric Pseudo Muscular Actuators and Pneumatic Muscle Actuators. *Mechatronics; an Internal Journal,* 10, 499–530.

Chou, C.-P. and Hannaford, B. (1996): Measurement and Modeling of McKibben Pneumatic Artificial Muscles. *IEEE Transactions on Robotics and Automation, 12,* 1, 90–102.

Prince, S. Xu, K. and Cheok, A. (2002): Augmented reality camera tracking with homographies. *IEEE Comput. Graph. Appl.* 22, 6, 39–45.

Zhang, Z. (2000): A Flexible New Technique for Camera Calibration. *IEEE Transactions on Pattern Analysis and Machine Intelligence,* 22, 11, 1330–1334.

## 6.2 Conference Proceedings:

Duca, F., Fredriksson. J. and Fjeld, M. (2007): Realtime 3D Hand Interaction: Single Webcam Low-Cost Approach. In *Workshop at the IEEE Virtual Reality 2007 Conference: Trends and Issues in Tracking for Virtual Environments,* 1–5.

Hirose, M., Hirota, K., Ogi, T., Hiroaki, Y., Kakehi, N., Saito, M. and Nakashige, M. (2001): HapticGEAR: The Development of a Wearable Force Display System for Immersive Projection Displays. In *Proceedings of the Virtual Reality 2001 Conference (VR'01),* IEEE, Yokohama, Japan, 123–129.

Iltanen, M. and Ellman, A. (2005): A low cost wearable force feedback device, fTouch. *2nd Intuition Workshop VR/VE & Industry: Challenge and opportunities*. Senlis, France 24–25.10.2005. 2 p (poster paper).

Iltanen, M. and Ellman, A. (2007): Wearable haptic device for an IPT system based on pneumatic muscles. *27th ASME Computers and Information in Engineering Conference,* IDETC/CIE, Las Vegas, Nevada, USA. (accepted for publication)

Jouppila, V. and Ellman, A. (2006): Multiplexed force control of pneumatic muscles. *ASME International Mechanical Engineering Congress and Exposition,* Chicago, Illinois, USA.

Mathieu, H. (2005): The Cyclope: A 6 DOF Optical Tracker Based on a Single Camera. *2nd INTUITION International Workshop*, Paris, France

Mulder, J.D., Jansen, J. and van Rhijn, A. (2003): An Affordable Optical Head Tracking System for Desktop VR/AR Systems. In *EGVE '03: Proceedings of the Workshop on Virtual Environments 2003,* ACM Press, New York, NY, USA, 215–223.

Woods, E., Mason, P. and Billinghurst, M. (2003): MagicMouse: an Inexpensive 6-Degree-of-Freedom Mouse. In *GRAPHITE '03: Proceedings of the 1st International Conference on Computer Graphics and Interactive Techniques in Australasia and South East Asia,* ACM Press, New York, NY, USA, 285–286.

ISBN-978-960-254-665-9


### 6.3 Internet Sources:

ARToolKit Home page. <URL: http://www.hitl.washington.edu/artoolkit/>, referenced 25.6.2007.

Festo. *Documentation — Fluidic muscle MAS-10- - - 534201* <URL: https://xdki.festo.com/xdki/data/doc_engb/PDF/EN/MAS_EN.PDF>, referenced 25.6.2007.

Immersion Co. *CyberGrasp™ Exoskeleton — Groundbreaking haptic interface for the entire hand*. <URL: http://www.immersion.com/3d/products/cyber_grasp.php>, referenced 20.6.2007.

Intel. *Open Source Computer Vision Library from Intel Corporation,* <URL: http://www.intel.com/technology/computing/opencv/>, referenced 5.7.2007.